Ni^{2+} affects dopamine uptake

which limits suitability as inhibitor of T-type voltage-gated Ca^{2+} channels

Katherine R. Brimblecombe[1*] and Stephanie J. Cragg[1,2]

[1]Department of Physiology, Anatomy and Genetics, Sherrington Building, and
[2]Oxford Parkinson's Disease Centre, University of Oxford, OX1 3PT, UK

***Corresponding author:**
Dr Katherine R Brimblecombe
Department of Physiology, Anatomy and Genetics
Sherrington Building
University of Oxford
OX1 3PT UK
E-mail: katherine.brimblecombe@dpag.ox.ac.uk

Number of figures: 5
Number of words for Abstract: 147
Total: 4711

Conflict of Interest: The authors declare that the research was conducted in the absence of any commercial or financial relationships that could be construed as a potential conflict of interest.

Acknowledgements
Funded by Parkinson's UK (Grant H-1003) and the Medical Research Council.

Abstract

Neuronal T-type voltage-gated Ca^{2+} channels are reported to have physiological roles that include regulation of burst firing, Ca^{2+} oscillations and neurotransmitter release. These roles are often exposed experimentally by blocking T-type channels with micromolar Ni^{2+}. We used Ni^{2+} to explore the role of axonal T-type channels in dopamine (DA) release in mouse striatum, but identified significant off-target effects on DA uptake. Ni^{2+} (100 µM) reversibly increased electrically evoked DA release and markedly extended its extracellular lifetime, detected using fast-scan cyclic voltammetry. Prior inhibition of the DA transporter (DAT) by cocaine (5 µM) occluded the facilitatory action of Ni^{2+} on DA release and conversely, allowed Ni^{2+} to inhibit release, presumably through T-channel inhibition. Ni^{2+} further prolonged the timecourse of DA clearance suggesting further inhibition of DA uptake. In summary, Ni^{2+} has major effects on DA transmission besides those due to T-channels that likely involve inhibition of the DAT.

Key words: Dopamine; Voltammetry; Ni^{2+}; T-type VGCC; Dopamine transporter

Introduction

Action potential-dependent opening of voltage-gated Ca^{2+} channels (VGCCs) facilitates the spatially and temporally organised delivery of Ca^{2+} that catalyses neurotransmission. Ten genes encode various pore-forming α_1 subunits of VGCCs, which can be grouped into 'high voltage-activated' channel types N, P, Q, R and L, or the 'low voltage-activated' T-type channels[1–3]. Specific pharmacological blockers can be used to identify the roles of specific VGCC subtypes. N, P,Q and R-type channels can be blocked with peptide toxins ω-conotoxin GVIA, ω-agatoxin IVA and SNX-482 respectively[4], L-type channels are blocked by dihydropyridines[5], and while there are some relatively selective inhibitors of T-type channels (e.g. NNC, mibefradil and TTA-P2 [6–8]), they are commonly blocked with Ni^{2+} at micromolar concentrations[9–11].

Neuronal T-type channels have been found to modulate a range of processes including low threshold spiking, burst firing through coupling with SK channels, and neuronal oscillations [10,12–16]. In addition to these well characterised roles, there are increasing reports that T-type channels control exocytosis [17–20]. The role of T-channels in the control of DA transmission has not been completely clarified. Striatal DA is crucial in the modulation of key neural circuits that control motor outputs and motivational behaviours, therefore understanding the mechanisms of DA release are important for a number of physiological and pathophysiological processes [21,22]. Previous studies have reported that N-, P-, Q- and T-type channels in striatum control DA release [11,23]. However, we and others recently identified that striatal DA transmission is under the powerful control of ACh released from cholinergic interneurons (ChI) which acts on nicotinic ACh receptors (nAChRs) on DA axons to modulate and drive DA release independently from activity in DA neurons [24–29]. Therefore, the previously proposed roles of T-type channels in the control of DA release may have arisen in part through striatal circuits that control ACh transmission, rather than through T-channels located on DA axons. T-type channels on DA axons have however been suggested to contribute to the release of GABA from striatal DA axons through some functional coupling to nAChR activation [30,31], but it is unclear whether T-type channels contribute to the release of DA, and whether this is restricted to periods of nAChR activation.

Here, we explored whether Ni^{2+} could be used to probe a role for T-type channels in striatal DA transmission, when the confounding effects of ACh inputs were prevented by inhibiting nAChRs. We identified surprising effects of Ni^{2+} on DA transmission that resemble those of DAT inhibition. Our data also offer support for some engagement of axonal T-channels in the processes regulating DA transmission. However, we show that the significant effect of Ni^{2+} on DA uptake rates are a major confounding factor, and will be so in all studies of other neuronal circuits and synapses where monoamine inputs are present and might contribute to experimental outcomes.

Results and Discussion

We explored the role of T-type VGCCs in the control of striatal DA release detected using fast-scan cyclic voltammetry at carbon-fibre microelectrodes in acute ex vivo slices of mouse brain. DA release was evoked electrically by brief stimulus pulses given singly (1p) as well as in short trains of 5 pulses at a large range of frequencies (5 to 100Hz). All experiments were conducted in the presence of the nAChR antagonist DHβE (1 µM) to eliminate confounding effects of striatal ACh. Under these control conditions, peak evoked extracellular DA concentration ($[DA]_o$) varied with stimulus frequency in CPu (**Figure 1a,** 1-way ANOVA, $F_{4,10}$=20.1, *p<0.001*) and in NAc (**Figure 1b**, 1-way ANOVA, $F_{4,10}$=50.5, *p<0.001*) as shown previously during nAChR inhibition [27,32,33]. Single pulses evoked a mean peak $[DA]_o$ of 0.62 ± 0.12 µM in CPu and 0.54 ± 0.08 µM in NAc, in line with previous studies [34,35].

The application of Ni^{2+} (100 µM) caused an unexpected increase in peak evoked $[DA]_o$ in CPu (**Figure 1a,** 2-way ANOVA $F_{1,20}$=10.7, *p<0.01*) and NAc (**Figure 1b,** 2-way ANOVA $F_{1,20}$=19.8, *p<0.001*) across stimulation types**.** Ni^{2+} did not modify the sensitivity of carbon fibre microelectrodes to DA in electrode calibration experiments (data not illustrated). The effects of Ni^{2+} on evoked DA release were reversible upon washout (**Figure 1c**). In addition to the increase in peak $[DA]_o$, Ni^{2+} also affected the timecourse of extracellular DA signals: Ni^{2+} delayed the time to peak, and extended the extracellular lifetime of the DA transients by slowing the extracellular clearance rate(**Figure 1a,b**). Curve fits to the decay phase of DA transients that were matched for concentration, as previously described [36], indicated that decay constants (*k*) for an exponential approximation to the curves were significantly lower with Ni^{2+} in CPu (**Figure 2a,** *k* values*:* 3.8 ± 0.1 s^{-1}, control vs. 1.9 ± 0.05 s^{-1}, Ni^{2+}; $F_{1,156}$=158, *p<0.001*) and NAc (**Figure 2b,** *k* values: 3.7 ± 0.2 s^{-1}, control vs. 1.8 ± 0.4 s^{-1}, Ni^{2+}; $F_{1,256}$=93.2, *p<0.001*). These changes in clearance rates correspond to an approximate doubling of half-lives of extracellular DA from 0.18 to 0.36 s in CPu and 0.19 to 0.38 s in NAc (**Figure 2a,b**).

The ability of Ni^{2+} to increase peak evoked $[DA]_o$, to delay the time to peak and extend the decay phase of DA transients are keeping with those expected of inhibitors of DA uptake via the DAT

[37–39]. Uptake through the DAT is the primary means of clearance of electrically evoked extracellular DA[40,41]. Cocaine (5 µM) is a broad spectrum monoamine uptake inhibitor but its effects on DA are primarily due to inhibition of the DAT[41,42] rather than other transporters. Cocaine, by inhibiting DA re-uptake should boost extracellular accumulation of DA and prolong DA extracellular lifetime, and furthermore, can also promote the releasability of DA through mobilising a synapsin-dependent pool [43,44] which increases the underlying DA release process itself. In our hands with these stimulation protocols and in the presence of nAChR inhibition, cocaine, like Ni^{2+}, increased peak evoked $[DA]_o$ in CPu (**Figure 3a,** 2-way ANOVA $F_{1,12}$=131 *p<0.001*) and NAc (**Figure 3b,** 2-way ANOVA $F_{1,12}$=37.0 *p<0.001*), prolonged the time to peak and slowed the decay phase of DA transients as predicted, similar to the effects of Ni^{2+}.

To investigate the hypothesis that Ni^{2+} was acting via an interaction with the DAT we applied Ni^{2+} after prior application of cocaine (5 µM). In the presence of cocaine, Ni^{2+} no longer increased peak evoked $[DA]_o$, but rather, Ni^{2+} decreased peak $[DA]_o$ evoked by 1p in CPu (**Figure 4a,** 2-way ANOVA $F_{1,12}$=11.9, *p<0.01;* 1p Bonferroni posttest *p<0.05*) and NAc (**Figure 4b,** 2-way ANOVA $F_{1,12}$=9.3, *p<0.05;* 1p Bonferroni posttest *p<0.05*). $[DA]_o$ evoked by 5-pulse trains, tested for 5 Hz and 100 Hz, was also reduced during the early rise phases consistent with a reduction in DA release. In other words, in the prior presence of cocaine, the ability of Ni^{2+} to boost DA release is diminished, but rather an ability to reduce is revealed, that is likely to be the T-channel dependence described previously [11]. However, an alternative explanation is that Ni^{2+} is enhancing the effect of cocaine, which at higher concentrations (30 µM) can decrease peak $[DA]_o$ [37]. The time for DA signals to peak and decay was further extended by Ni^{2+} compared to cocaine alone (**Figure 4a,b**). Curve fits to the decay phase of DA transients that were matched for concentration, indicated that decay constants (*k*) for an exponential approximation to the curves were significantly lower with Ni^{2+}, after discrete single pulse stimuli (1p) or a pulse train at high frequency (5p 100 Hz) in CPu (**Figure 5a,** *k* values: 1.03 ± 0.03 s^{-1}, control, vs 0.51 ± 0.02 s^{-1}, Ni^{2+}; $F_{1,312}$=138, *p<0.001*) and NAc (**Figure 5b,** *k* values: 0.83 ± 0.07 s^{-1}, control, vs 0.36 ± 0.01 s^{-1}, Ni^{2+}; $F_{1,402}$=605, *p<0.001*). These changes corresponded to an

approximate doubling of half-lives of extracellular DA from 0.67 to 1.36 s in CPu and 0.84 to 1.90 s in NAc (**Figure 5a,b**), consistent with further scope for limiting DA uptake to rates slower than resulting from 5 μM cocaine alone[37].

The roles of T-type VGCCs are routinely explored using micromolar concentrations of Ni^{2+}. However, the data presented here indicate that these concentrations of Ni^{2+} have major off-target effects that modulate DA signals. Ni^{2+} appears to be affecting DA transmission via inhibition of DAT: Ni^{2+} increased the peak evoked $[DA]_o$, and the time to peak, and slowed the decay phase of DA transients in an analogous manner to the enhanced release and reduced uptake seen after DAT inhibition by cocaine. When DAT function was compromised by prior application of cocaine, Ni^{2+} decreased DA release, consistent with an inhibition of T-type channels shown previously (when ACh was not controlled for)[11], although we cannot rule out a potentiation of cocaine's inhibitory effects on DA release at high concentrations[37]. Many cations have been shown to interact with the DAT, the best characterised of which is Zn^{2+} [45–47]. DAT has at least three ion binding sites, and occupation of these sites affects a number of parameters of DAT function including DA uptake and the efficacy of DAT blockers including cocaine[46]. Zn^{2+} has been shown to directly inhibit DA uptake[47,48], but to the best of our knowledge the effects of Ni^{2+} directly on DAT have not been explored. Ni^{2+} has however been demonstrated to modify the action of DAT uptake blockers: Ni^{2+} has been shown to both increase and decrease DAT blocker binding[45,47] although its precise mode of action is unresolved.

DAT inhibition by cocaine did not eradicate the full effects of Ni^{2+}. Ni^{2+} additional effects on DA clearance might be additive with effects of cocaine on the DAT or might be potentiating the effects of cocaine, which are submaximal at 5 μM, but this was not the focus of this current study. It is difficult to work with higher, more 'maximal' concentrations since cocaine has other effects at higher concentrations such as inhibition of Na^+ channels and nAChRs[49–51]. It remains possible that Ni^{2+} inhibits DA clearance through multiple mechanisms including other unresolved mechanisms that are independent of the DAT.

A role for T-type VGCCs is increasingly being appreciated in neuronal and synaptic physiology. However, Ni^{2+}, a tool commonly used to block and explore T-type roles has profound consequences for DA function that appear to be at least in part due to inhibition of the DAT. It is not yet known whether this action extends to other monoamine transporters and transmitters. In any event, these data identify that Ni^{2+} can dramatically enhance DA signalling, a finding which should be used to re-evaluate the potential functions of T-channels identified elsewhere. Substantial changes to local DA function are to be expected after Ni^{2+} administration. Ni^{2+} is therefore not a suitable tool for probing the roles of T-type VGCCs in experimental paradigms where DA transmission could influence interpretation of results. Instead drugs including mibefradil, NNC 55-0396 and TTA-P2 may be better suited as selective T-type channel blockers, although their individual limitations should also be considered.

Methods

Slice preparation

Male adult mice were C57 Bl6/J wild-types (Charles River), or dopamine transporter (DAT)-Cre heterozygote mice described previously [24]. Mice were killed by cervical dislocation, the brains removed, and 300 µm coronal slices containing CPu and NAc prepared as described previously [24,33] in ice-cold HEPES-based buffer saturated with 95% O_2/5% CO_2, containing in mM: 120 NaCl, 20 $NaHCO_3$, 6.7 HEPES acid, 5 KCl, 3.3 HEPES salt, 2 $CaCl_2$, 2 $MgSO_4$, 1.2 KH_2PO_4, 10 glucose. Slices were incubated at room temperature for ≥ 1 hour in saturated HEPES-based buffer before transferral to recording chamber.

Fast-scan cyclic voltammetry (FCV)

DA release was monitored in ex vivo slices using FCV as we have described previously [24,33]. Slices were superfused in a recording chamber with bicarbonate-buffered artificial cerebrospinal fluid (aCSF) saturated with 95%O_2/5%CO_2 at 31–33°C, containing in mM: 124 NaCl, 26 $NaHCO_3$, 3.8 KCl,

2.4 $CaCl_2$, 1.3 $MgSO_4$, 1.3 KH_2PO_4, 10 glucose. Evoked extracellular DA concentration ($[DA]_o$) was monitored using fast-scan cyclic voltammetry (FCV) at 7-10 µm diameter carbon-fibre microelectrodes (CFM) fabricated in house (tip length 50-100 µm) and a Millar voltammeter (Julian Millar, Barts and the London School of Medicine and Dentistry). In brief, a triangular voltage waveform (range -700 mV to +1300 mV vs. Ag/AgCl) was applied at 800 V/s at a scan frequency of 8 Hz. Electrodes were switched out of circuit between scans. Electrodes were calibrated using 1-2 µM DA in each experimental medium. Calibration solutions were made immediately prior to calibration from a 2.5 mM stock solution in 0.1 M $HClO_4$ stored at 4°C. Signals were attributable to DA by the potentials for peak oxidation and reduction currents (oxidation peak: +500-600 mV, reduction peak: ~-200 mV).

Electrical stimulation

Recordings were obtained from both dorsolateral CPu and NAc. DA release was evoked by a local bipolar concentric Pt/Ir electrode (25 µm diameter; FHC inc. ME, USA) placed approximately 100 µm from the CFM. Stimulus pulses (200 µs duration) were generated at perimaximal current (0.6 mA). DA neurons *in vivo* exhibit a range of firing frequencies from ~1-40 Hz or higher. We applied pulses singly (1p) or in 5-pulse trains at 5, 25, 40 and 100 Hz. Mean peak $[DA]_o$ evoked by 1p was equivalent to that of a 1 Hz train; 1p is used in frequency comparisons to indicate maximum 1 Hz data. A frequency of 100 Hz is useful for exploring changes differences in short-term plasticity that arise through changes in initial DA release probability [27]. Electrical stimulations were repeated at 2.5 minute intervals.

All data were recorded in the presence of the nAChR antagonist, dihydro-β-erythroidine (DHβE; 1µM), to remove the confounding effects of VGCCs on cholinergic interneurons that regulate ACh release, and its subsequent effects on DA release. Muscarinic ACh receptors (mAChRs) do not regulate DA transmission during the stimulation protocols used here [35] and therefore it was not necessary to include an mAChR antagonist. Release was TTX sensitive (data not shown), and was not modulated by glutamate or GABA antagonists as shown previously (Threlfell et al., 2010).

Drugs and solutions

Dihydro-β-erythroidine (DHβE) was purchase from Tocris. $NiCl_2$ and cocaine was purchased from Sigma Aldrich. Stock solutions of DHβE, Ni^{2+} and cocaine were dissolved in dH_2O to 1000-2000x final concentrations and stored at -20°C. Drugs were diluted to final concentrations in aCSF immediately prior to use and were applied in the superfusion solution.

Data and statistical analysis

Data were acquired and analysed using Axoscope 10.2 (Molecular devices) or Whole Cell Programme (WCP; University of Strathclyde, Glasgow) and Excel macros written locally. Data are expressed as mean ± standard error of the mean (SEM), and n = number of animals. Data from each animal were obtained by averaging at least 3 recordings for each stimulus type in a given recording site, and normalising to mean control 1p conditions for each animal. Population means of peak evoked $[DA]_o$ were compared using one- or two-way ANOVA with post-hoc Bonferroni's t-test where appropriate, using GraphPad Prism. DA transients were analysed using 2-way ANOVA with post-hoc Bonferroni's to identify the time points which differed between drug conditions.

DA uptake was investigated by fitting exponential decay curves to concentration-matched transients and comparing the decay constant (*k*) between curves. Curves were assessed for two concentration ranges (note: *k* and half-life parameters for any given drug condition were not statistically different between curves fitted for different concentration ranges). Parametric tests were used because raw control data passed Shapiro-Wilk normality test.

References

(1) Catterall, W. A. (2000) Structure and regulation of voltage-gated Ca2+ channels. *Annu. Rev. Cell Dev. Biol. 16*, 521–55.

(2) Tsien, R. W., and Barret, C. F. (2000) A Brief History of Calcium Channel Discovery. Landes Bioscience.

(3) Catterall, W. A. (2011) Voltage-gated calcium channels. *Cold Spring Harb. Perspect. Biol. 3*, a003947.

(4) Catterall, W. A., Perez-Reyes, E., Snutch, T. P., and Striessnig, J. (2005) International Union of Pharmacology. XLVIII. Nomenclature and structure-function relationships of voltage-gated calcium channels. *Pharmacol. Rev. 57*, 411–25.

(5) Lipscombe, D., Helton, T. D., and Xu, W. (2004) L-type calcium channels: the low down. *J. Neurophysiol. 92*, 2633–41.

(6) Li, M., Hansen, J. B., Huang, L., Keyser, B. M., and Taylor, J. T. (2005) Towards selective antagonists of T-type calcium channels: design, characterization and potential applications of NNC 55-0396. *Cardiovasc. Drug Rev. 23*, 173–96.

(7) Choe, W., Messinger, R. B., Leach, E., Eckle, V.-S., Obradovic, A., Salajegheh, R., Jevtovic-Todorovic, V., and Todorovic, S. M. (2011) TTA-P2 is a potent and selective blocker of T-type calcium channels in rat sensory neurons and a novel antinociceptive agent. *Mol. Pharmacol. 80*, 900–10.

(8) Martin, R. L., Lee, J.-H., Cribbs, L. L., Perez-Reyes, E., and Hanck, D. A. (2000) Mibefradil Block of Cloned T-Type Calcium Channels. *J. Pharmacol. Exp. Ther. 295*, 302–308.

(9) Zamponi, G. W., Bourinet, E., and Snutch, T. P. (1996) Nickel block of a family of neuronal calcium channels: subtype- and subunit-dependent action at multiple sites. *J. Membr. Biol. 151*, 77–90.

(10) Wolfart, J., and Roeper, J. (2002) Selective Coupling of T-Type Calcium Channels to SK Potassium Channels Prevents Intrinsic Bursting in Dopaminergic Midbrain Neurons. *J. Neurosci. 22*, 3404–3413.

(11) Chen, B. T., Moran, K. A., Avshalumov, M. V, and Rice, M. E. (2006) Limited regulation of somatodendritic dopamine release by voltage-sensitive Ca channels contrasted with strong regulation of axonal dopamine release. *J. Neurochem. 96*, 645–55.

(12) Markram, H., and Sakmann, B. (1994) Calcium transients in dendrites of neocortical neurons evoked by single subthreshold excitatory postsynaptic potentials via low-voltage-activated calcium channels. *Proc. Natl. Acad. Sci. 91*, 5207–5211.

(13) Chevalier, M., Lory, P., Mironneau, C., Macrez, N., and Quignard, J.-F. (2006) T-type CaV3.3 calcium channels produce spontaneous low-threshold action potentials and intracellular calcium oscillations. *Eur. J. Neurosci. 23*, 2321–9.

(14) Cui, G., Okamoto, T., and Morikawa, H. (2004) Spontaneous opening of T-type Ca2+ channels contributes to the irregular firing of dopamine neurons in neonatal rats. *J. Neurosci. 24*, 11079–87.

(15) Bender, K. J., Uebele, V. N., Renger, J. J., and Trussell, L. O. (2012) Control of firing patterns through modulation of axon initial segment T-type calcium channels. *J. Physiol. 590*, 109–18.

(16) Jarvis, S. E. (2000) G Protein Modulation of N-type Calcium Channels Is Facilitated by Physical Interactions between Syntaxin 1A and Gbeta gamma. *J. Biol. Chem. 275*, 6388–6394.

(17) Carbone, E., Giancippoli, A., Marcantoni, A., Guido, D., and Carabelli, V. (2006) A new role for T-type channels in fast "low-threshold" exocytosis. *Cell Calcium 40*, 147–54.

(18) Pan, Z. H., Hu, H. J., Perring, P., and Andrade, R. (2001) T-type Ca(2+) channels mediate neurotransmitter release in retinal bipolar cells. *Neuron 32*, 89–98.

(19) Weiss, N., Hameed, S., Fernandez-Fernandez, J. M., Fablet, K., Karmazinova, M., Poillot, C., Proft, J., Chen, L., Bidaud, I., Monteil, A., Huc-Brandt, S., Lacinova, L., Lory, P., Zamponi, G. W., and De Waard, M. (2012) A Cav3.2/syntaxin-1A signaling complex controls T-type channel activity and low-threshold exocytosis. *J. Biol. Chem. 287*, 2810–2818.

(20) Cueni, L., Canepari, M., Adelman, J. P., and Lüthi, A. (2009) Ca(2+) signaling by T-type Ca(2+) channels in neurons. *Pflugers Arch. 457*, 1161–72.

(21) Gerfen, C. R., and Surmeier, D. J. (2010) Modulation of Striatal Projection Systems by Dopamine. *Annu. Rev. Neurosci. 34*, 441–66.

(22) Rice, M. E., Patel, J. C., and Cragg, S. J. (2011) Dopamine release in the basal ganglia. *Neuroscience 198*, 112–37.

(23) Phillips, P. E., and Stamford, J. A. (2000) Differential recruitment of N-, P- and Q-type voltage-operated calcium channels in striatal dopamine release evoked by "regular" and "burst" firing. *Brain Res. 884*, 139–46.

(24) Threlfell, S., Lalic, T., Platt, N. J., Jennings, K. A., Deisseroth, K., and Cragg, S. J. (2012) Striatal dopamine release is triggered by synchronized activity in cholinergic interneurons. *Neuron 75*, 58–64.

(25) Cachope, R., Mateo, Y., Mathur, B. N., Irving, J., Wang, H.-L., Morales, M., Lovinger, D. M., and Cheer, J. F. (2012) Selective activation of cholinergic interneurons enhances accumbal phasic dopamine release: setting the tone for reward processing. *Cell Rep. 2*, 33–41.

(26) Zhou, F. M., Liang, Y., and Dani, J. A. (2001) Endogenous nicotinic cholinergic activity regulates dopamine release in the striatum. *Nat. Neurosci. 4*, 1224–9.

(27) Rice, M. E., and Cragg, S. J. (2004) Nicotine amplifies reward-related dopamine signals in striatum. *Nat. Neurosci. 7*, 583–4.

(28) Zhang, H., and Sulzer, D. (2004) Frequency-dependent modulation of dopamine release by nicotine. *Nat. Neurosci. 7*, 581–2.

(29) Cragg, S. J. (2006) Meaningful silences: how dopamine listens to the ACh pause. *Trends Neurosci. 29*, 125–31.

(30) Tang, A.-H., Karson, M. A., Nagode, D. A., McIntosh, J. M., Uebele, V. N., Renger, J. J., Klugmann, M., Milner, T. A., and Alger, B. E. (2011) Nerve terminal nicotinic acetylcholine receptors initiate quantal GABA release from perisomatic interneurons by activating axonal T-type (Cav3) Ca^{2+} channels and Ca^{2+} release from stores. *J. Neurosci. 31*, 13546–61.

(31) Nelson, A. B., Hammack, N., Yang, C. F., Shah, N. M., Seal, R. P., and Kreitzer, A. C. (2014) Striatal cholinergic interneurons Drive GABA release from dopamine terminals. *Neuron 82*, 63–70.

(32) Exley, R., and Cragg, S. J. (2008) Presynaptic nicotinic receptors: a dynamic and diverse cholinergic filter of striatal dopamine neurotransmission. *Br. J. Pharmacol. 153 Suppl*, S283–97.

(33) Exley, R., McIntosh, J. M., Marks, M. J., Maskos, U., and Cragg, S. J. (2012) Striatal α5 nicotinic receptor subunit regulates dopamine transmission in dorsal striatum. *J. Neurosci. 32*, 2352–6.

(34) Hartung, H., Threlfell, S., and Cragg, S. J. (2011) Nitric oxide donors enhance the frequency dependence of dopamine release in nucleus accumbens. *Neuropsychopharmacology 36*, 1811–22.

(35) Threlfell, S., Clements, M. A., Khodai, T., Pienaar, I. S., Exley, R., Wess, J., and Cragg, S. J. (2010) Striatal muscarinic receptors promote activity dependence of dopamine transmission via distinct receptor subtypes on cholinergic interneurons in ventral versus dorsal striatum. *J. Neurosci. 30*, 3398–408.

(36) Anwar, S., Peters, O., Millership, S., Ninkina, N., Doig, N., Connor-Robson, N., Threlfell, S., Kooner, G., Deacon, R. M., Bannerman, D. M., Bolam, J. P., Chandra, S. S., Cragg, S. J., Wade-Martins, R., and Buchman, V. L. (2011) Functional alterations to the nigrostriatal system in mice lacking all three members of the synuclein family. *J. Neurosci. 31*, 7264–74.

(37) John, C. E., and Jones, S. R. (2007) Voltammetric characterization of the effect of monoamine uptake inhibitors and releasers on dopamine and serotonin uptake in mouse caudate-putamen and substantia nigra slices. *Neuropharmacology 52*, 1596–605.

(38) Chen, B. T., and Rice, M. E. (2001) Novel Ca2+ dependence and time course of somatodendritic dopamine release: substantia nigra versus striatum. *J. Neurosci. 21*, 7841–7.

(39) Cragg, S. J., Hille, C. J., and Greenfield, S. A. (2000) Dopamine Release and Uptake Dynamics within Nonhuman Primate Striatum In Vitro. *J. Neurosci. 20*, 8209–8217.

(40) Cragg, S. J., and Rice, M. E. (2004) DAncing past the DAT at a DA synapse. *Trends Neurosci. 27*, 270–7.

(41) Giros, B., Jaber, M., Jones, S. R., Wightman, R. M., and Caron, M. G. (1996) Hyperlocomotion and indifference to cocaine and amphetamine in mice lacking the dopamine transporter. *Nature 379*, 606–12.

(42) Budygin, E. A., John, C. E., Mateo, Y., and Jones, S. R. (2002) Lack of cocaine effect on dopamine clearance in the core and shell of the nucleus accumbens of dopamine transporter knock-out mice. *J. Neurosci. 22*, RC222.

(43) Kile, B. M., Guillot, T. S., Venton, B. J., Wetsel, W. C., Augustine, G. J., and Wightman, R. M. (2010) Synapsins differentially control dopamine and serotonin release. *J. Neurosci. 30*, 9762–70.

(44) Venton, B. J., Seipel, A. T., Phillips, P. E. M., Wetsel, W. C., Gitler, D., Greengard, P., Augustine, G. J., and Wightman, R. M. (2006) Cocaine increases dopamine release by mobilization of a synapsin-dependent reserve pool. *J. Neurosci. 26*, 3206–9.

(45) Bonnet, J. J., Benmansour, S., Amejdki-Chab, N., and Costentin, J. (1994) Effect of CH3HgCl and several transition metals on the dopamine neuronal carrier; peculiar behaviour of Zn2+. *Eur. J. Pharmacol. 266*, 87–97.

(46) Bonnet, J.-J. (2003) Interactions of cations and anions with the binding of uptake blockers to the dopamine transporter. *Eur. J. Pharmacol. 479*, 199–212.

(47) Richfield, E. (1993) Zinc modulation of drug binding, cocaine affinity states, and dopamine uptake on the dopamine uptake complex. *Mol. Pharmacol. 43*, 100–108.

(48) Loland, C. J., Norregaard, L., Litman, T., and Gether, U. (2002) Generation of an activating Zn(2+) switch in the dopamine transporter: mutation of an intracellular tyrosine constitutively alters the conformational equilibrium of the transport cycle. *Proc. Natl. Acad. Sci. U. S. A. 99*, 1683–8.

(49) Damaj, M. I., Slemmer, J. E., Carroll, F. I., and Martin, B. R. (1999) Pharmacological characterization of nicotine's interaction with cocaine and cocaine analogs. *J. Pharmacol. Exp. Ther. 289*, 1229–36.

(50) Francis, M. M., Vazquez, R. W., Papke, R. L., and Oswald, R. E. (2000) Subtype-selective inhibition of neuronal nicotinic acetylcholine receptors by cocaine is determined by the alpha4 and beta4 subunits. *Mol. Pharmacol. 58*, 109–19.

(51) O'Leary, M. E., and Chahine, M. (2002) Cocaine binds to a common site on open and inactivated human heart (Na(v)1.5) sodium channels. *J. Physiol. 541*, 701–16.

Figure legends

Figure 1. Ni^{2+} reversibly increases $[DA]_o$ and DA extracellular lifetime.

(**a, b**) Mean profiles of $[DA]_o$ ± SEM vs time evoked by 1 or 5 pulses (5-100 Hz) in (a) CPu or (b) NAc under control conditions or the presence of Ni^{2+} (100 µM). Data are normalised to 1p peak $[DA]_o$ in control conditions. *Inset*, cyclic voltammograms of evoked DA release in control conditions (*black*) or with Ni^{2+} (*red*). * p<0.05, **p<0.01, ***p<0.001 Bonferroni post-test between control and Ni^{2+} at 0.125 s intervals. **(c)** Peak $[DA]_o$ evoked by 1p as Ni^{2+} is washed on (*black bar*) and off. The nAChR inhibitor DHβE (1 µM) was present throughout. N=3.

Figure 2. Ni^{2+} increases the half-life of evoked $[DA]_o$

(**a, b**) Exponential curve fit to the decay phases of DA transients that are matched for concentration, following 1p or 5p 100Hz in CPu (**a**)and NAc (**b**) in control conditions (*black*) and in Ni^{2+} (*red*) (*dotted lines*, 95% confidence limits). Dashed lines are half-lives. The nAChR inhibitor DHβE (1 µM) was present throughout. N=3.

Figure 3. DA uptake inhibition by cocaine increases $[DA]_o$ and DA extracellular lifetime.

(a,b) Mean profiles of $[DA]_o$ ± SEM vs time evoked by 1 or 5 pulses (5-100 Hz) in (a) CPu or (c) NAc in control conditions (DHβE, 1 µM) or after the addition of cocaine (5 µM). Data are normalised to 1p peak $[DA]_o$ in control conditions. Control conditions (black lines), cocaine (blue lines). * p<0.05 **p<0.01, ***p<0.001 Bonferroni posttest between control and Ni^{2+} at 0.125 s intervals. N=3.

Figure 4. Ni^{2+} reduces DA release when DAT is inhibited, and extends extracellular DA lifetime.

(**a, b**) Mean profiles of $[DA]_o$ ± SEM vs time evoked by 1 or 5 pulses (5-100 Hz) in (a) CPu or (b) NAc in the presence of cocaine (5 µM) (*black*) or cocaine+Ni^{2+} (100 µM) (*red*). Data are normalised to 1p

peak $[DA]_o$ in cocaine conditions. *p<0.05 **p<0.01, ***p<0.001 Bonferroni post-test between cocaine and Ni^{2+} at 0.125 s intervals. DHβE (1 μM) was present throughout. N=3.

Figure 5. Ni^{2+} increases the half-life of evoked $[DA]_o$ when DAT is inhibited

(**a, b**) Exponential curve fit to the decay phases of DA transients matched for concentration, following 1p or 5p 100Hz in CPu (**a**) and NAc (**b**) in cocaine (*black*) or cocaine+Ni^{2+} (*red*) (*dotted lines*, 95% confidence limits). *Dashed lines* are half-lives. DHβE (1 μM) was present throughout. N=3.

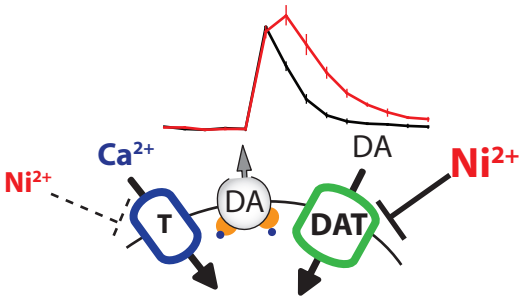
Ca2+
Ni2+
T
DA
DA
DAT
Ni2+

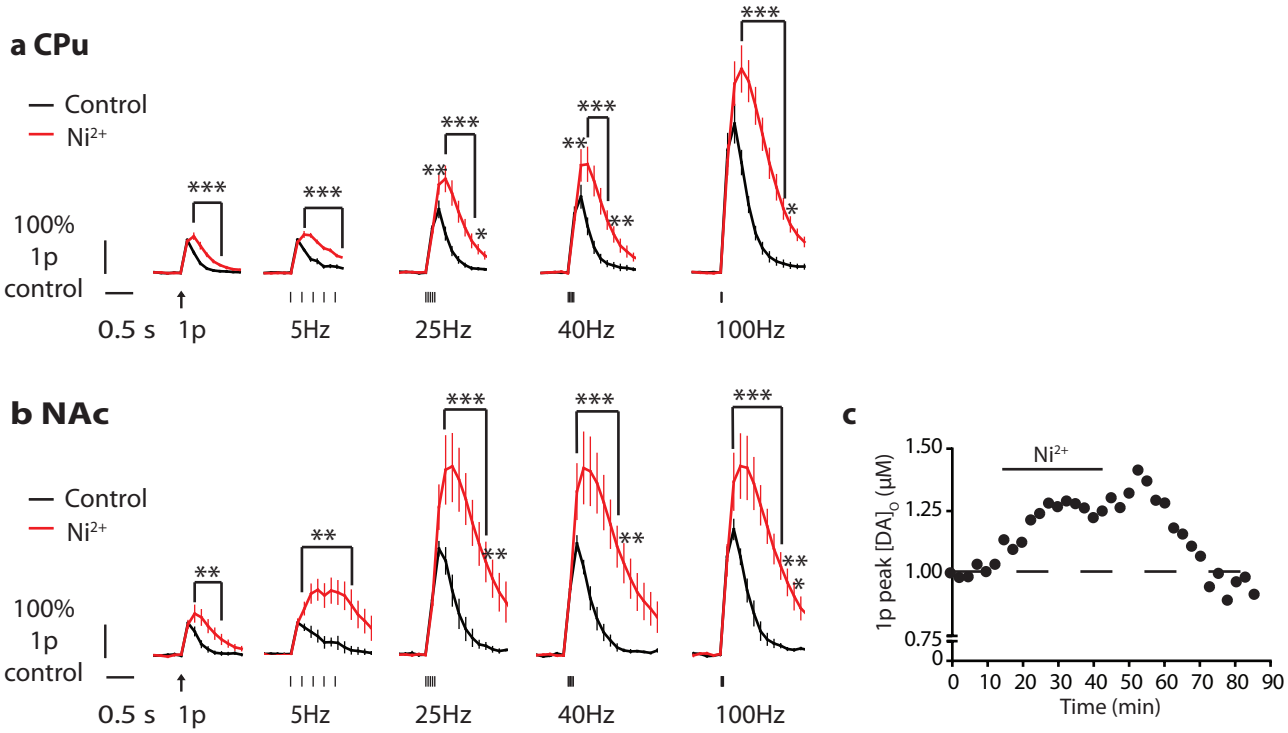

Figure 1 Brimblecombe and Cragg

a CPu

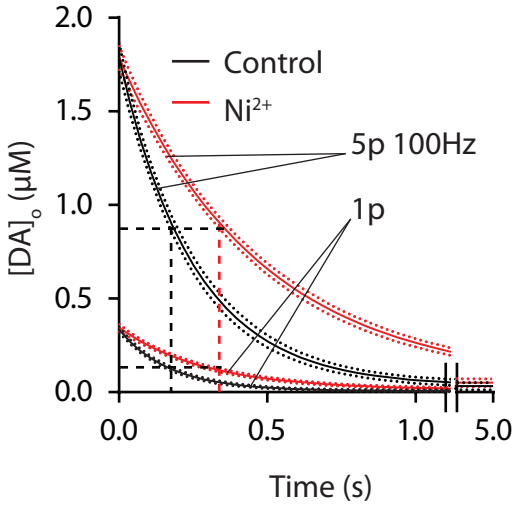

b NAc

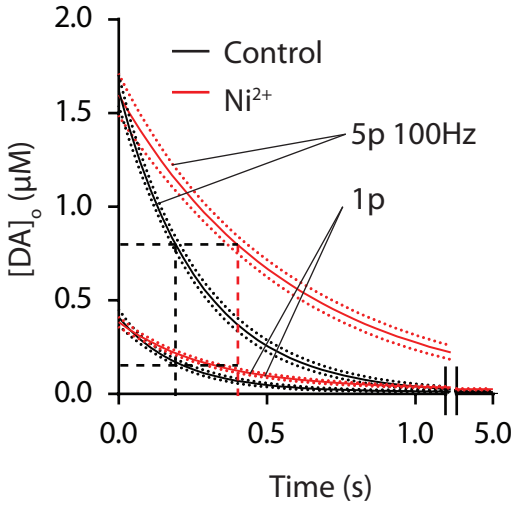

Figure 2 Brimblecombe and Cragg

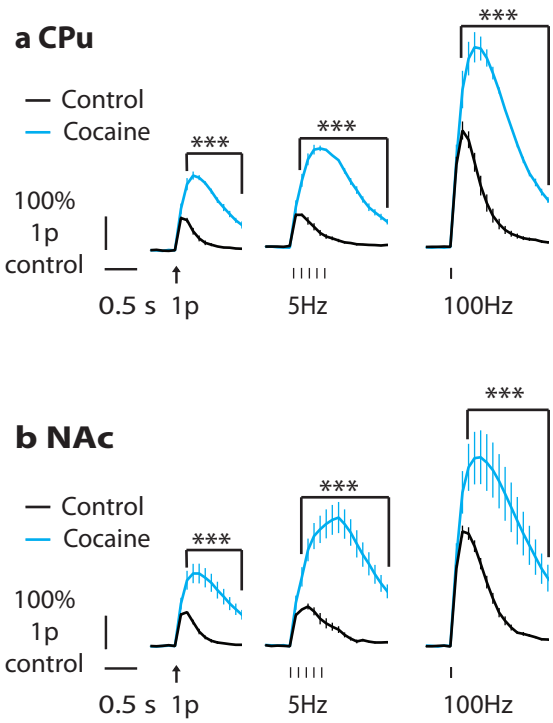

Figure 3 Brimblecombe and Cragg

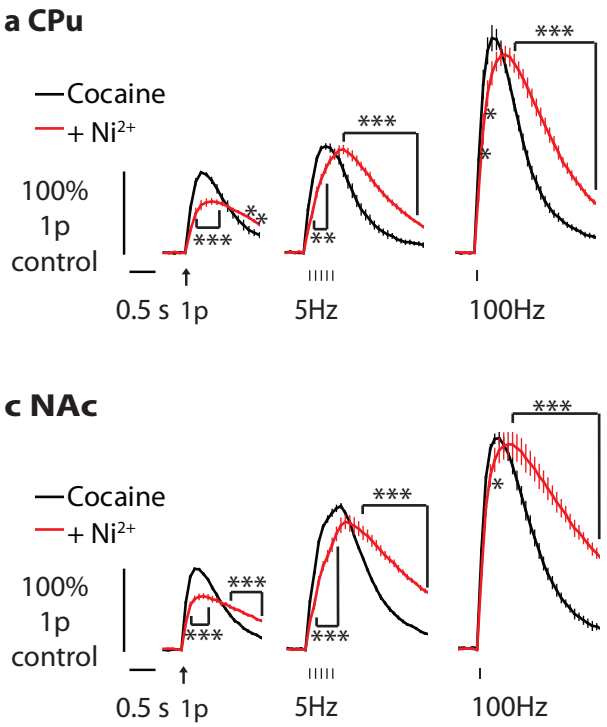

Figure 4 Brimblecombe and Cragg

a CPu

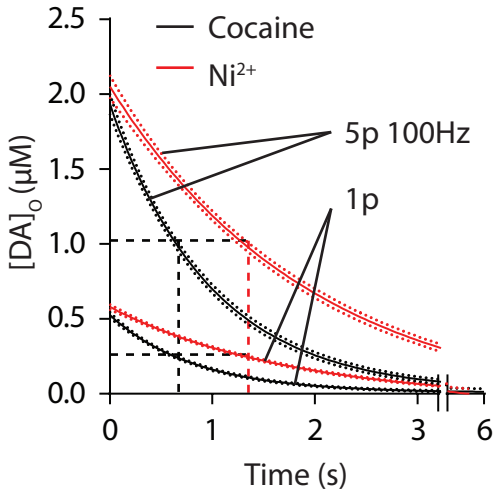

b NAc

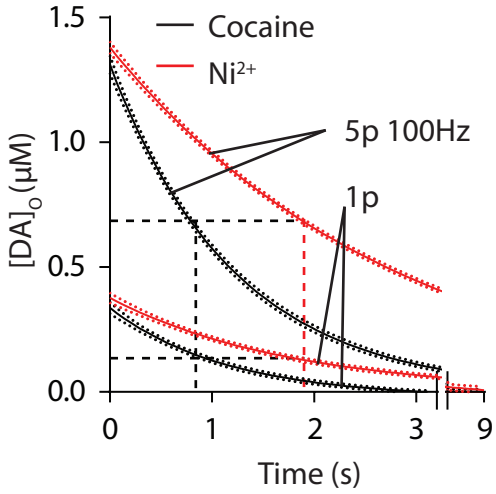

Figure 5 Brimblecombe and Cragg